COMPRESSION CURVE OF A FIBROUS COMPOSITE

S. T. Mileiko and A. A. Khvostunkov

UDC 539.3

Results are presented of an experimental investigation of a single-directional fibrous composite under compression in the bonding direction. The buckling modes are detected: the customary bending and a shear mode which holds for comparatively low sample flexibilities.

1. An experimental determination of the mechanical properties of materials under compression has a number of peculiarities which sometimes make obtaining reliable results difficult. Firstly, the comparatively short working length of the sample makes the stress state far from uniform, and measurement of the displacements less reliable than in the case of tension. An increase in the working length results in sample buckling. Additional peculiarities can appear in the compression of fibrous materials.

Firstly, the buckling of the system of bonding fibers in the matrix is possible. An energy stability criterion is applied in [1] to a plane model of a composite, and it is shown that for low armature concentrations, buckling of the system of rigid bounding planes is energetically suitable such that any two adjacent planes buckle out of phase, tension–compression in a direction perpendicular to the fundamental compression is imposed on the fundamental stress state of the matrix. As the percentage of bonding increases, buckling of the bonding system in one phase becomes more favorable, hence, shear is imposed on the fundamental state of the matrix. Practically the same result has been obtained in [2] by using a static criterion. The cophasal buckling mode should apparently be more characteristic for ordinary combinations of the properties of the components and the magnitudes of the volume fractions of the armature. An expression for the critical stress in the bonding element has been obtained for this case in [1, 2],

$$\sigma_*' = \frac{G_m}{v_f v_m} \tag{1.1}$$

where G is the shear modulus and v the volume fraction of the component. (Here and below the subscript f refers to the armature, the subscript m and the double prime to the matrix, while the quantities without subscripts or primes are averages referring to the composite as a whole.)

No rigorous experimental verification of (1.1) has apparently been made since reconstruction of the test model and conditions used in the test in [1, 2] is difficult. A comparison between the experimental results in [3] and (1.1) is not justified since the stresses it yields simply cannot be realized by the armature used in [3]. The test conditions of aluminum samples bonded with a stainless wire and the buckling mode observed in [4] are not perfectly clear, and the authors' interpretation of their results is arbitrary to a significant degree.

Secondly, growth of the initial imperfections of the armature [5] occurs under compression, which results in a diminution of the effective elastic modulus of the composite.

The main idea used in the experiments following below is that the samples in the compression tests should be considered as a certain structure. But it is expedient to vary some structural parameter in studying the structure, the flexibility, say, in the case of a compressed rod. As will be shown below, this will result in a natural determination of the material.

2. Several years ago, Yu. N. Rabotnov expressed the idea about the expediency of determining the tangential modulus of a material under compression from experiments on the stability of rods. Indeed, experi-

Moscow. Translated from Zhurnal Prikladnoi Mekhaniki i Tekhnicheskoi Fiziki, No. 4, pp. 155-160, July-August, 1971. Original article submitted February 12, 1971.

TABLE 1

d/l	σ_*, kg/mm^2	μ	$E_k \cdot 10^{-3}$ kg/mm^2
0.0281	14.2	0.495	7.26
0.0337	18.9	0.515	6.75
0.0421	24.3	—	5.56
0.0562	30.9	—	3.99
0.0843	35.3	—	1.65

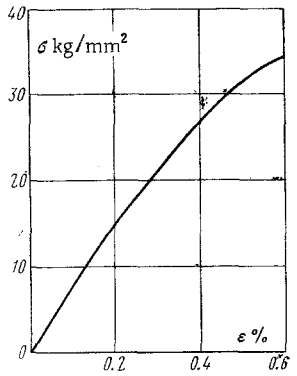

Fig. 1

ments yield critical loads close to the quantities obtained by the tangential modulus formula [6]. Therefore, compression testing rods of diverse flexibility under fixed support conditions and then determining the tangent modulus as a function of the stress can reproduce the strain curve under compression when the dependence obtained is integrated. The degree of correspondence between this $\sigma-\varepsilon$ curve and the true compression curve will be the same as the degree of correspondence between the tangential modular load and the actual critical load of the compressed rod. But it should be noted that using the compression characteristics of the material requires namely its tangent modulus in many cases, and numerical differentiation of the experimental $\sigma-\varepsilon$ dependence is, as a rule, fraught with great errors.

Thus, a homogeneous (or quasi-homogeneous) rod of length l is compressed by an increasing stress σ. According to Shanley, the rod buckling will occur at the stress

$$\sigma_* = \left(\frac{\pi i}{\mu l}\right)^2 E_k \qquad \left(E_k = \frac{d\sigma}{d\varepsilon}\right) \tag{2.1}$$

Here i is the minimal radius of inertia of a rod section, μ is a coefficient dependent on the rod support conditions, and E_k is the tangential modulus of the rod material at the stress σ_*.

Rigid framing of the rod with small deviations from the rectilinear can be realized comparatively easily in experiment by compressing the sample with flat endfaces perpendicular to its axis between plane-parallel slabs.

Indeed, a d = 16.84 mm diameter bar of D16T was compressed in this manner in preliminary tests. If the elastic modulus is taken as $E = 7.1 \cdot 10^3$ kg/mm^2, then the values of μ obtained in the first two rows of the table can be considered to correspond to rigid framing ($\mu = 0.5$). Values of the tangent modulus E_k, taking into account $\mu = 0.5$, are determined in the last column of this table. After interpolation and integration, the compression curve (Fig. 1) of the tested duraluminum, whose yield point under tension is ~ 55 kg/mm^2, is constructed from these data. (The dashes are given in the table since the tangent modulus is known to be less than the elastic modulus in the appropriate lines.)

3. The subject investigated herein is an aluminum-stainless steel wire composite. Aluminum A5 aluminum foil was used as matrix, and chromium-nickel wire* of the armature had a 0.11 mm diameter and tension yield point of ~ 240 kg/mm^2. The method of producing the composite was by diffusion welding in a vacuum. The welding regime was 525°C temperature, 3 kg/mm^2 pressure for 30 min, and a vacuum on the order of $5 \cdot 10^{-5}$ torr. After the original wire had been heated in the welding regime its strength dropped negligibly and was ~ 230 kg/mm^2. The billet under welding was obtained by winding the wire on a layer of foil, where the relationships between the wire diameter, the foil spacing, and thickness were selected for a given bonding percentage v_f so as to obtain a uniform, almost hexagonal armature distribution in cross section. Examples of the wire distributions obtained in the composite cross sections are shown in Fig. 2a (for a volume fraction $v_f = 0.095$) and in Fig. 2b ($v_f = 0.440$). The dimensions of the card obtained after welding were $2 \times 35 \times 100$ mm^3.

The samples were cut on an electric spark tool with subsequent careful grinding of the side surfaces and endfaces in order to assure their mutual perpendicularity. The average size of a sample cross section was 2×6 mm^2. The ratio l/h of the length to the thickness of the samples varied between 4 and 50. The samples were tested on a ZD-40 machine with a ~ 2 kg/mm$^2 \cdot$ sec loading rate.

4. Three buckling modes were observed. The ordinary bending mode is characteristic for samples with high flexibility (Fig. 3a). As the flexibility decreases, the nature of the buckling changes, the sample

*The wire was obtained from the laboratory of the A. A. Klekovkin Belorets Metallurgical Combine.

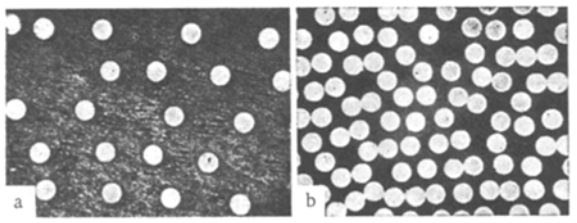

Fig. 2

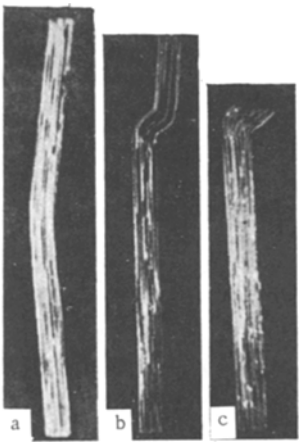

Fig. 3

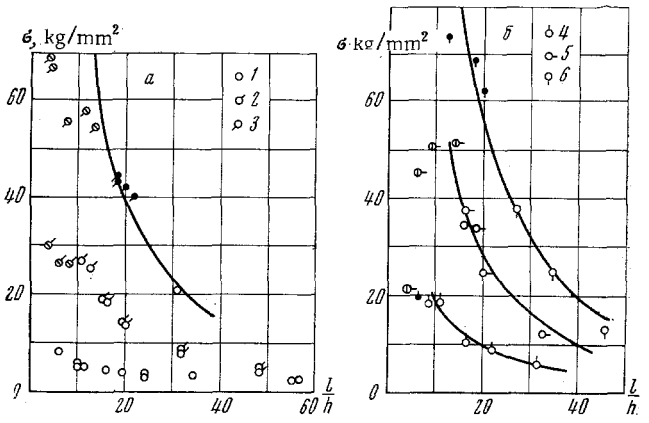

Fig. 4

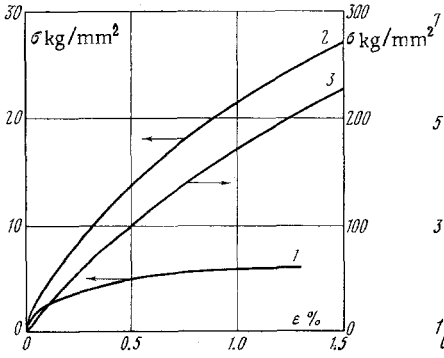

Fig. 5

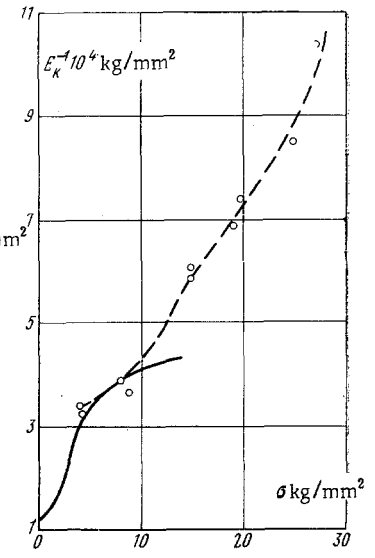

Fig. 6

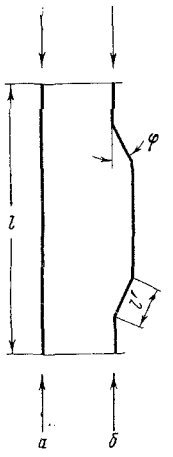

Fig. 7

snaps with the formation of steps in whose zone shear occurs in the material of the matrix (Fig. 3b). The shear is localized at the sample enface (Fig. 3c) in still shorter samples.

The dependence of the critical stress σ_* on the parameter l/h which characterizes the sample flexibility, is presented in Fig. 4. The points 1, 2, 3 in Fig. 4a correspond to the volume fractions $v_f = 0$, 0.095, and 0.305. The points 4, 5, 6 in Fig. 4b correspond to the volume fractions 0.058, 0.215, and 0.440. The open circles refer to the bending buckling mode, the dark circles to the shear mode, and the lined circles to shear at the endfaces. The passage from the bending mode to the shear mode occurs for greater values of l/h, the smaller the magnitude of the volume fraction v_f.

Let us first examine just those results which refer to the bending buckling mode. Assuming the sample quasi-uniform, let us consider (2.1) to be valid. Let us also assume that the strain curve of the composite in that section where there are still no localized zones of the kind shown in Figs. 4b and c is obtained by the simple rule of mixtures, i.e.,

$$\sigma = \sigma' v_f + \sigma'' v_m \tag{4.1}$$

where σ' and σ'' are functions of the strains $\varepsilon = \varepsilon' = \varepsilon''$, characteristic for the fiber and matrix under uniaxial loading. This means that the influence of normal stresses is not taken into account here in planes perpendicular to the sample axis, which are on the order of the square of the difference between the Poisson ratios of the components [7], and the influence of the armature on the plastic properties of the matrix, noted in [8], for example,* is neglected. The first assumption is justified by the smallness of the corrections obtained, as is illustrated by calculations of the appropriate elastic moduli. The second assumption apparently does not roughen the real picture since the diameter of the bonding fibers is sufficiently large in this case, in contrast to [8].

Now, using (2.1) and the data presented in Fig. 3, let us construct the dependence of E_k^{-1} on the stresses for the matrix. Let us take $E = 7.1 \cdot 10^3$ kg/mm^2 as the elastic modulus of the matrix (the point $\sigma = 0$). Integrating

$$\frac{dE}{d\sigma} = E_k^{-1}(\sigma)$$

we find the strain curve of the matrix under compression (Fig. 5, curve 1). Furthermore, in these same $E_k^{-1} - \sigma$ coordinates, let us superpose experimental points for the composite $v_f = 0.095$ (Fig. 6). We determine the initial part of the curve (solid line) by means of (4.1) by taking the matrix compression curve obtained and an elastic wire with the modulus $E = 2.1 \cdot 10^4$ kg/mm^2. Starting with $\sigma = 8$ kg/mm^2, let us integrate numerically and reproduce the composite compression curve. This is shown in Fig. 5 (curve 2). Furthermore, applying (4.1) to the matrix and composite deformation curves, we find the wire compression curve (Fig. 5, curve 3).

By using (4.1) the compression curve of a composite with a given armature content can be obtained. Knowledge of the compression curve rapidly yields the dependence of the critical stability stress on the parameter l/h. The computed curves obtained are superposed in Fig. 4 by solid lines. As is seen, the experimental points for the bending buckling mode agree well with the appropriate computed curves.

5. Now, let us turn to the shear buckling mode. The shape of the samples (Fig. 3b) suggests the path of analysis here. As is ordinarily done, let us examine a plane composite model. Let us consider the armature to be linearly elastic with modulus E_f, and the matrix to be ideally plastic with yield point σ_m. Let us determine the energy of uniform axial compression (Fig. 7a). For sufficiently high mean stresses σ in the composite ($\sigma \gg \sigma_m$) it will be

$$U_1 = \frac{\sigma^2}{2E_f v_f} l \tag{5.1}$$

per unit cross-sectional area.

* Let us note that the electron microscope investigation of the Al–Fe composite in [4] does not disclose the influence of bonding on the dislocation structure of the deformed aluminum matrix.

Assuming a possible shape of the elastic line of the sample as shown in Fig. 7b with four plastic hinges in the armature and plastic shears $\gamma'' = \varphi$ of the matrix in the rectilinear portions of length l of the composite, and with unloaded vertical "linkages" of the sample, let us write the energy of this state in the form

$$U_2 = \sigma_m \varphi v_m l' \tag{5.2}$$

The work of the localized strain in the plastic hinges is not taken into account in (5.2).

Considering the transition from the first state into the second to occur without a change in the spacing between the sample endfaces, we have

$$l' = \frac{\sigma}{E_f v_f} \frac{l}{4(\sin {}^1/_2 \varphi)^2}$$

and assuming $U_1 = U_2$, we obtain the critical shear angle

$$\varphi_* = 2 \frac{\sigma_m}{\sigma} v_m \tag{5.3}$$

The expression obtained is valid only for small φ; it shows that for each sufficiently large stress governed by the external load, there exists a "broken-line" state with break angle φ_* in addition to the fundamental rectilinear state. But for $\varphi < \varphi_*$ the energy of the broken-line state will be greater than the energy of the rectilinear state, i.e., it is necessary to overcome some potential barrier for the shear buckling mode. In other words, the sample cannot take the broken-line mode without a jolt from outside.

Growth of the initial sample imperfections can be such a jolt. Let the rod have the elastic line

$$y_0 = \frac{a_0}{2}\left(1 - \cos \frac{2\pi x}{l}\right) \tag{5.4}$$

in the initial state, where a_0 is a small deflection at $x = {}^1/_2 l$.

Following the usual procedure of integrating the longitudinal bending equations, we easily arrive at the dependence of the additional deflection function $y(x)$ on the external load σ

$$y = \frac{a_0}{1 - \sigma/\sigma_*} \sin^2 \frac{\pi x}{l}$$

Here σ_* is given by (2.1). Furthermore, neglecting the initial curvature of the rod we obtain that for stresses σ_{**} the maximum angle of rotation of the rod at $x = {}^1/_4 l$, $x = {}^3/_4 l$ turns out to be the critical angle φ_* for the same stress

$$\left.\frac{dy}{dx}\right|_{x={}^1/_4 l} = \pi \frac{a_0}{l} \frac{1}{1 - \sigma_{**}/\sigma_*} = \varphi_* = 2 \frac{\sigma_m}{\sigma_{**}} v_m$$

The rod goes over into the broken-line state for a stress σ_{**} such that

$$\frac{\sigma_{**}}{\sigma_*} = \left[1 + \frac{\pi}{2} \frac{a_0}{h} \frac{h}{l} \frac{\sigma_*}{\sigma_m} \frac{1}{v_m}\right]^{-1} \tag{5.5}$$

If the magnitude of the initial imperfection a_0/h is assumed constant for a given batch of the samples, then the deviation of the dependence of the critical stress σ_{**} from the curve computed by means of the bending mode will be greatest in the domain of low values of l/h. As v_f grows this deviation will also increase. This is in qualitative agreement with the test results presented in Fig. 3. The value of a_0/h which results in quantities σ_{**}/σ_* obtained in test is ~ 0.05; this probably does not differ too much from real values of the effective initial imperfection.

The values of the critical stresses for the bending and shear buckling modes agree within the spread of the test data if the ratio l/h is sufficiently large. Hence, the actual buckling mode can be determined by peculiarities of the experiment, and certainly, by discrepancies between the model and the real material. For example, if the endfaces of the compressed sample are fastened in screws, then rigid framing is conserved for larger deflections and the shear buckling mode is developed for larger l/h. Shear in the sample endfaces under compression is apparently a distorted end effect of the shear buckling mode.

The authors are grateful to V. P. Gryaznov for assistance in preparing the samples.

LITERATURE CITED

1. B. W. Rosen, "Mechanics of composite strengthening." Fiber Composite Mater., Amer. Soc. Metals, Ohio (1965).
2. W.-Y. Chung and R. B. Testa, "The elastic stability of fibers in a composite plate," J. Composite Mater., 3, No. 1 (1969).
3. E. M. Ferran and B. Harris, "Compression strength of polyester resin reinforced with steel wires," J. Composite Mater., 4, No. 1 (1970).
4. M. R. Pinnel and A. Lawley, "Correlation of uniaxial yielding and substructure in aluminum–stainless steel composites," Metall. Trans., 1, No. 5 (1970).
5. B. P. Makarov and G. V. Arutyunyan, "On the influence of random curvatures of the armature on the physicomechanical characteristics of composites," Trudy Moskovsk. Énerg. In-ta, No. 74 (1970).
6. Yu. N. Rabotnov, Strength of Materials [in Russian], Fizmatgiz, Moscow (1962).
7. R. Hill, "Elastic properties of reinforced solids: some theoretical principles," J. Mech. Phys. Solids, 11, No. 5 (1963).
8. A. Kelly and H. Lilholt, "Stress–strain curve of a fibre-reinforced composite," Phil. Mag., 20, No. 164 (1969).